Vital sign monitoring: a practical solution by a MR-compatible phonocardiography interferometric probe

J. NEDOMA[a], S. KEPAK[a], J. CUBIK[a], J. FRNDA[b], M. DURICA[b], M. FAJKUS[a], R. MARTINEK[c]

aDepartment of Telecommunications, Faculty of Electrical Engineering and Computer Science, VSB - Technical University of Ostrava, 17 listopadu 15/2172, 708 33 Ostrava, Czech Republic
bDepartment of Quantitative Methods and Economic Informatics, Faculty of Operation and Economics of Transport and Communications, University of Zilina, Univerzitna 1, 010 26 Zilina, Slovakia
cDepartment of Cybernetics and Biomedical Engineering, Faculty of Electrical Engineering and Computer Science, VSB - Technical University of Ostrava, 17. listopadu 15/2172, 708 33 Ostrava, Czech Republic

This paper deals with the description of S_1-S_1 interval detection of the phonocardiographic signal obtained by a fiber-optic Mach-Zehnder interferometer. A non-invasive measuring probe encapsulated in a bicomponent (base and catalyst) entitled Zhermack ZA 50 LT was designed. The probe is immune to the electromagnetic interferences (EMI) and therefore can be operated under strong magnetic fields. The laboratory results (obtained from 8 volunteers) were compared to the reference electrocardiograph (ECG) signal and evaluated by an objective Bland-Altman (B-A) method. Based on the results, it is possible to say that the S_1-S_1 interval detection with the presented fiber-optic interferometric probe is as reliable as the measurement of time between the R-R wave of the ECG signal since the B-A analysis resulted in 95.59 % samples laid in ± 1.96 SD. The test carried out in a real Magnetic Resonance Imaging (MRI) environment demonstrated that the presence of the probe in the MRI scanner does not affect the quality of this imaging modality. The developed sensor can be suitable for cardiac triggering.

1. Introduction

The electrical signals of cardiac activity are nowadays recorded by electrocardiograph (ECG). The curve, corresponding to the electrical activity of the heart is used to determine the heart rate. ECG is now widely used and is one of the basic non-invasive investigative methods in cardiology [1]. In the beginning, ECG used to have three electrical leads; nowadays, the standard ECG has twelve leads [2]. In addition to the electrocardiogram, different variables such as acoustic signal, changes in blood pressure in the circulatory system, changes in tissue volume as a result of volume changes in the circulatory system, changes in tissue impedance associated with changes in blood volume in a given section of tissue, or changes in blood flow velocity as consequence of changes in blood pressure in the circulatory system [3-6] are used to determine heart rate.

Since one of the consequences of heart activity is also acoustic waves and mechanical vibrations, they can be monitored by listening (auscultation) or special microphones with the possibility to emphasize certain frequencies in the phonographic record (phonocardiogram) [7]. Acoustic-mechanical manifestations of cardiac activity are associated with cardiac wall vibrations and valve closures during the heart's beat. One way is to use Fiber Bragg gratings (FBG). These can be embedded in the wearable elastic textiles [8] compatible with magnetic resonance (MR) [9]. FBG probe can also be mounted on the diaphragm leading to the excellent compliance to the reference stethoscope [10]. Similarly, a minimal relative measurement error was found in the study [11], which focused on using the FBG sensor to measure the ballistographic signal.

The most sensitive methods to monitor acoustic-mechanical responses of the heart is the use of fiber-optic interferometers. The principle of the function is to measure changes in the light wave path due to the action of the forces acting on the fiber from the external environment. In the case of interferometers, these changes can be measured with high accuracy at a value level smaller than the wavelength of the light. The sensitivity is so high that a range of measurements can also be performed in indirect contact with the human body (e.g., a layer of textile may be placed between the probe and the body).

Publications that describe the use of interferometric sensors for heart rate monitoring or S wave detection can be found in [12-26]. Between the most interesting prior works can include papers [12] and [23]. In paper [12] a heartbeat from an optical interferometric signal by using convolution kernel compensation (CKC) latent variable analysis (LVA) approach is examined. The obtained efficiency (sensitivity of 97.8 ± 3.0 %, the precision of 93.6 ± 7.6 %) and accuracy (reference-to-detected beat delay of 167 ± 65 ms) are within acceptable limits indicating that unobtrusive heartbeat detection using the proposed approach is feasible. Paper [23] described a 24 GHz Six-Port microwave interferometer could be used to

detect the current heart rate of a person-under-test as the reference authors used a commercial ECG product. The mean heart rate determined by the microwave interferometer was 59.5 bpm and thereby only 0.3 bpm higher than the mean heart rate detected by the ECG measurement (59.2 bpm). This confirms the functionality of the proposed routine together with the Six-Port microwave interferometer.

The paper is primarily focused on S_1-S_1 interval detection using the combination of the cheapest two-arm Mach-Zehnder fiber interferometer and the interferometric probe encapsulation in the RTV silicon rubber. The encapsulation material entitled as Zhermack ZA 50 LT was used which is a bicomponent (base and catalyst) addition RTV silicon rubber that vulcanizes at room temperature [27]. System and probe design offer several beneficial properties for biomedical applications such as electromagnetic interference (EMI) resistance and electrical non-conductivity. This type of probe can be used, for example, to monitor heart rate in the harsh environments, typically magnetic resonance, where it can serve as a detector of hyperventilation conditions typically occurring in tight MR environments. The test carried out in a real MRI environment (1.5T MR scanner) demonstrated that the presence of the probe in the MRI scanner does not affect the quality of this imaging modality.

Thanks to this can be probe used in the cardiac triggering - synchronization of MR signal acquisition to the cardiac or respiratory cycle, which is a very solved issue today [28]. Cardiac contractions can be detected by ECG or a peripheral pulse transducer. During cardiac examinations, the patient's ECG signal is measured to trigger scans to the cardiac cycle. The principal source of artifacts in the ECG due to the presence of the magnetic field itself is called the magnetohydrodynamic effect. It can cause a false QRS detection in certain R- wave detection algorithms leading to false triggers. However, the fiber-optic sensors operate on a different principle, and their operation is not affected by the magnetic field.

2. Methods

The activity of the heart is connected with the creation of a large number of characteristic sounds. These sounds occur due to changes in the velocity (or the character) of the blood flow and closing or opening of the respective valves. Hence, this is a diagnostic method that is based on sensing the acoustic signals (heart sounds) described above, which accompany the mechanical vibrations originating in the heart and the blood vessels.

The PCG signal consists of two major sound phenomena: the first one, the so-called systolic sounds (S_1), and, the second one, the so-called diastolic sounds (S_2), please see Fig. 1. The first sound (S_1) is associated with the closure of the bicuspid and tricuspid valves at the beginning of the systole, and its commencement corresponds to the ECG R-wave peak. The second sound (S_2) is induced by the closure of the semilunar valves. The

formation and duration of the diastolic sound (S_2) is associated with the ECG T-wave.
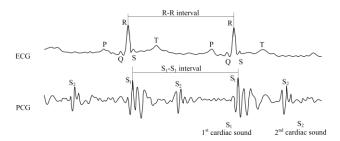

Fig. 1. Sample recording representing ECG and PCG signals

The principle of heart rate measurement using the interferometric probe is based on the so-called interferometric phonocardiography (IPCG). Acoustic and mechanical activity of the heart and the mechanical functioning of the lungs cause changes in the core refractive index and changes in the length of the measuring optical fiber placed on the human body and these microscopic changes in the optical path are appear in the phase delay of ϕ and its difference $\Delta\phi$, please see following equation:

$$\phi = \frac{2\pi n}{\lambda}\Delta L + \frac{2\pi}{\lambda}L\Delta n - 2\pi L \frac{n}{\lambda^2}\Delta\lambda \qquad (1)$$

where λ is the wavelength of the radiation source, n the refractive index of the optical fiber core, L is the physical length of the fiber.

Photo of the interferometric probe is shown in Fig. 2. The proposed probe used in experiments is made using a

2 m optical fiber loop in a 900 μm tube having a radius of 6-8 cm and the total weight of the probe is 43 g. We used FC (APC) connectors because they are designed for high-vibration environments and minimal back reflections. The angled physical contact allows the surfaces of two connected fibers to be in direct contact with each other and because the fiber end is polished at an angle to prevent reflected light from traveling back up the fiber.

Fig. 2. Proposed interferometric measuring probe

Signal processing is shown in Fig. 3. A bandpass filter of 20 to 80 Hz was designed for HR determination, wherein the filter frequencies are based on the knowledge of the interferometric sensors found in [18]. The filter type used was the 3rd order Butterworth. Peaks are detected above this signal. The heart rate is calculated using the following relation $HR = 60/(t_n - t_{n-1})$, where t_n is the time mark of the n_{th} peak and t_{n-1} is the time mark of the preceding peak. A median filter with window size 6 is used for smoothing the heart rate over time.
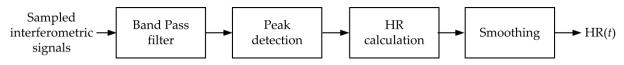

Fig. 3. Schematic diagram of the signal processing from the interferometric probe

3. Experimental setup and results

The experimental measurements were provided with the written informed consents of 8 volunteers (test subjects) of both sexes (five men: M_1-M_5, and three women: F_1-F_3) in a research laboratory. The test subjects were between 21 and 67 years of age, their height was between 157 to 204 cm, and their body mass was between 48 to 119 kilograms. The interferometric sensor was placed on the chest (around the pulmonic area) and fixed by a contact elastic strap to the human body. The subjects were tested in the supine position in a relaxed state because we assume the use of the sensor for patients with minimal body movements (long-term ill patients or patients in the harsh magnetic environment). The experimental part is based on the evaluation of the short-time sequences (summary: 1 hour and 21 minutes of measured data). Measurement scheme is shown in Fig. 4.
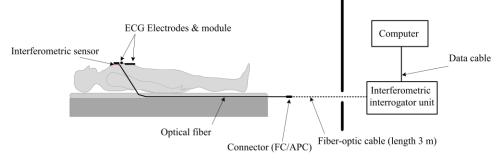

Fig. 4. Graphical and schematic diagram of the measurement

A three-lead electrocardiography (ECG) device (NI ELVIS, National Instruments) was used as a reference for monitoring the heart rate (HR) of the tested volunteers. Interferometric interrogator uses a light source laser (type MCLS1 Thorlabs, wavelength 1550 nm) with a reference power of 3 mW. Further a photodetector (Thorlabs PDA10CS-EC, InGaAs 700-1800 nm), the signal is then sampled by the National Instruments 6210 measuring module, which is supported in the LabVIEW development environment (National Instruments), which was used to create a custom application that performed data recording, filtration, and HR extraction functions. For our experimental tests, we used a sampling rate of 10 kHz based on our previous research [29-30].

Acquired data were compared by the objective Bland-Altman method [31]. The Bland-Altman analysis is a numerical and graphical method to compare two measurements techniques (reference and interferometric sensor). In this method, the differences between the two techniques are plotted against the averages of the two techniques. [32, 33].

Fig. 5 shows an example of a 3-second time window, which represents the heart activity of test subject M1 against the reference three-lead electrocardiography (ECG) device. The individual maxima detected in the case of the ECG signal represent the R wave, in the case of the signal obtained from our probe, the individual maxima detected characterize the S1 wave (the S1 wave is a characteristic of the R wave of the ECG signal), please see Fig. 1. Also, the detected S_1-S_1 interval is plotted, this graphical representation confirms the theoretical assumptions given in section 2. The y-axis in the case of an ECG signal represents the voltage (mV), in the case of the interferometric probe, the y-axis also represents voltage (V) with adequate overall power for the collected light – i.e., the phase from the photodetector.
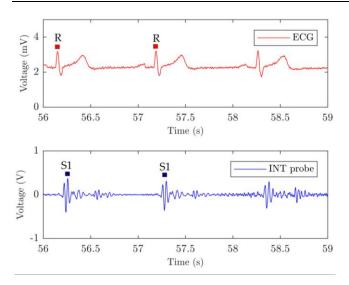
Fig. 5. An example of a 3-second time window (detection of S_1-S_1 interval and R-R interval)

Fig. 6 shows the 30 seconds of the signal recorded from the male volunteer against the reference ECG device. It can be seen from the graphs that the signals from the probe designed by us correlate with the signal from ECG. This fact is confirmed by the B-A method and detailed described in Table 1 which contains the statistical data obtained from all 8 test volunteers. Time (s) represents the total measurement time for the subject, the AHR represents the average heart rate (beat per minute) of the test volunteers, NoS represents the number of samples obtained by interferometric probe, Error means the absolute number of samples that are outside the ±1.96 Standard deviation (SD) range and Rel. Error indicates the number of faulty samples relative to the total number of samples expressed in percent.
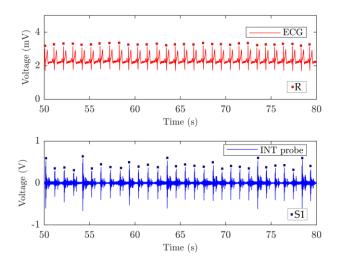

Fig. 6. An example of a long 30-second time window, which represents the heart activity of test subject M_1 against the reference three-lead electrocardiography (ECG) device

The key experimental results are summarized in Table 1. The "Rec. time" of individual test volunteers is represented in seconds, "AHR" means average heart rate, "NoS" means the number of detected maxims and "Samples in ±1.96 SD" represents results of Bland-Altman analysis expressed in %. The results obtained with the Bland-Altman analysis demonstrated the functionality of the FBG sensor (95.59 %). We can also see that relative error is below 5 % for all measurements.

4. Discussion

The relative error of the interferometric probe is below 5 %. Despite the good value, we must emphasize that the probe is designed primarily for the monitoring rather than diagnostics. Achieved results are comparable to other fiber-optic technologies such as FBGs. In [33] authors presented FBG probe with 94.88 % agreement to the reference ECG which is a very close performance to our interferometric probe. Bending sensors can provide interesting results and MRI-compatibility as well [34]. Authors presented a smart cushion with the microbending sensor embedded. Compared to the commercial pulse oximetry the microbending sensor has shown good accuracy with detection error up to 8 %. Sensor mat mentioned in [35] had a correlation coefficient of 0.997.

The benefits of the proposed interferometric system and probe include the possibility of remote evaluation of the HR measured. The distance (interrogator unit - probe) is limited by the used type of interconnecting optical fiber (fiber attenuation coefficient) and, further, by the power of the radiation source used (we used the laser with the output power of 3 mW, but this value can be higher not affection the measurement results). Another benefit is the simplicity of the interrogation unit which is using regular optical power detectors.

The reference arm is stored as part of the interrogator unit and for the encapsulation a polystyrene foam was used based on our previous research [36].

The functionality of the proposed system and probe was verified by a series of experimental measurements of basic vital signs and authors are ready to carry out a long-term detailed analysis of proposed sensor in the follow-up research. We are currently awaiting the permission of the ethics committee to carry out extensive clinical trials.

Volunteers can carry out slight body movements (minor and major artifacts) like a slight movement or trembling of the legs, torso rotation, slight hand movement, head movement, rapid breathing or coughing. If these artifacts occur, the signal may be negatively affected and the error rate in the evaluation may be increased (we must emphasize all of the different artifacts during measurements are taken into account in the results described above regarding the efficiency of the probe). As for individual artifacts, some of the minor artifacts (shallow breathing, head movement, etc.) did not distort the HR measurements, but some major artifacts like the rotation of torso caused degradation of the signal. In the follow-up research, we are ready to carry out a detailed

analysis of the influence of the minor/major artifacts. However, we must emphasize that this requires long-time extensive independent research. Every movement of the patient is individual, and it is difficult to ensure the reproducibility of the research.

The test carried out in a real Magnetic Resonance Imaging (MRI) environment demonstrated that the presence of the probe in the MRI scanner does not affect the quality of this imaging modality. The interferometric is transparent to the MRI system and based on the acquired results we were able to verify that the probe (location of the probe is red marked on Figure 7) does not introduce any artifacts into the spin-echo (SE) T1-weighted, please see Fig. 7.

Fig. 7. MRI image acquired from the probe location: sagittal view (512 x 512resolution)

Table 1. Summary of the measurements

Subject	Rec. Time (s)	AHR (bpm)	NoS (-)	Error (-)	Rel. Error (%)	Samples in ± 1.96 SD (%)
M_1	608	64	643	23	3.58	96.42
M_2	621	72	734	28	3.81	96.19
M_3	613	74	742	31	4.18	95.82
M_4	607	68	684	27	3.95	96.05
M_5	608	73	739	39	5.28	94.72
F_1	611	77	782	42	5.37	94.63
F_2	609	79	793	38	4.79	95.21
F_3	608	81	814	35	4.30	95.70
Summary	**4 885**	**-**	**5 931**	**263**	**4.41**	**95.59**

5. Conclusion

This paper is focused on the description of the S_1-S_1 interval detection of PCG signal obtained using the proposed and laboratory-tested probe based on the fiber-optic Mach-Zehnder interferometer. The IPCG signal consists of two major sound phenomena: the first one, the so-called systolic sounds (S_1), and the second, the so-called diastolic sounds (S_2). The primary initial (S_1) is associated with the closure of the bicuspid and tricuspid valves at the beginning of the systole, and its commencement corresponds to the ECG R-wave peak. As the results from laboratory measurements shown, this type of sensor can be used as a possible replacement for an ECG to determine the heart rate of the human body, because B-A analysis resulted in 95.59 % samples laid in ± 1.96 SD. The test carried out in a real Magnetic Resonance Imaging (MRI) environment demonstrated that the

presence of the probe in the MRI scanner does not affect the quality of this imaging modality. The sensor developed and the detection methods described have proven suitable for the cardiac triggering. The team of authors is now trying to link the trigger systems of MRI with the fiber-optic sensing system and to make comparisons with existing triggering systems of established MRI manufacturers.

References

[1] J. D. Shopp, L. K. Stewart, T. W. Emmett, J. A. Kline, Academic Emergency Medicine **22**, 1127 (2015).

[2] M. Zabel, B. Acar, T. Klingenheben, M. R. Franz, S. H. Hohnloser, M. Malik, Circulation **102**, 1252 (2000).

[3] L. Biel, O. Pettersson, L. Philipson, P. Wide, IEEE Transactions on Instrumentation and Measurement **50**, 808 (2001).

[4] S. Tamaki, T. Yamada, Y. Okuyama, T. Morita, S. Sanada, Y. Tsukamoto, M. Hori, Journal of the American College of Cardiology **53**, 426 (2009).

[5] R. Ogura, Y. Hiasa, T. Takahashi, K. Yamaguchi, K. Fujiwara, Y. Ohara, S. Hosokawa, Circulation journal **67**, 687 (2003).

[6] G. Chen, S. A. Imtiaz, E. Aguilar-Pelaez, E. Rodriguez-Villegas, Healthcare Technology Letters **2**, 28 (2015).

[7] S. Ismail, I. Siddiqi, U. Akram, Eurasip Journal on Advances in Signal Processing, 1 (2018).

[8] D. L. Presti, C. Massaroni, D. Formica, P. Saccomandi, F. Giurazza, M. A. Caponero, E. Schena, IEEE Sensors Journal **17**(18), 6037 (2017).

[9] C. Massaroni, P. Saccomandi, D. Formica, D. Lo Presti, M. A. Caponero, G. Di Tomaso, F. Giurazza, E. Muto, IEEE Sensors Journal **16,** (22) 8103 (2016).

[10] K. Chethana, A. S. Guru Prasad, S. N. Omkar, S. Asokan, Journal of biophotonics **10,** 2 (2017).

[11] L. Dziuda, F. W. Skibniewski, Biocybern. Biomed. Eng. **34,** 101 (2014).

[12] A. A. Sepehri, A. Gharehbaghi, T. Dutoit, A. Kocharian, A. Kiani, Computer Methods and Programs in Biomedicine **99**, 43 (2010).

[13] S. Sprager, A. Holobar, D. Zazula, Biosignals – Proceedings of the International Conference on Bio-Inspired Systems and Signal Processing, 396 (2013).

[14] C. Will, K. Shi, F. Lurz, R. Weigel, A. Koelpin, International Symposium on Intelligent Signal Processing and Communication Systems, 483 (2015).

[15] S. Hong, W. Jung, T. Kim, K. Oh, Journal of Lightwave Technology **36**, 974 (2018).

[16] P. Podbreznik, D. Đonlagic, D. Lesnik, B. Cigale, D. Zazula, Zdravniski Vestnik **83**, 901 (2014)

[17] P. Podbreznik, D. Onlagic, D. Lesnik, B. Cigale, D. Zazula, Journal of Biomedical Optics, **18,** 10 (2013).

[18] S. Sprager, D. Zazula, Proc. IEEE Transactions on Biomedical Engineering **59**(10), 2922 (2012).

[19] M. Y. M. Noor, G. Rajan, G. D. Peng, IEEE Sensors Journal **14**, 1154 (2014).

[20] S. Sprager, D. Donlagic, D. Zazula, Proceedings of the IASTED International Conference on Signal and Image Processing, 280 (2011).

[21] P. Varady, T. Micsik, S. Benedek, Z. Benyo, IEEE Transactions on Biomedical Engineering **49**, 936 (2002).

[22] S. Sprager, D. Zazula, Computer Methods and Programs in Biomedicine **111**, 41 (2013).

[23] C. Will, K. Shi, F. Lurz, R. Weigel, A. Koelpin, International Symposium on Intelligent Signal Processing and Communication Systems, 483 (2015).

[24] H. L. Byeong, H. K. Young, S. P. Kwan, B. E. Joo, J. K. Myoung, S. R. Byung, Y. C. Hae, Sensors, **12**, 2467 (2012).

[25] Y. H. Hsieh, N. K. Chen, 6th IEEE/International Conference on Advanced Infocomm Technology (ICAIT), Hsinchu, 113 (2013).

[26] D. Zazula, S. Sprager, Proceedings of the Symposium on Neural Network Applications in Electrical Engineering, 171 (2012).

[27] Product. Available online: http://www.jacomp.fi/wp-content/uploads/2017/12/ZA50LT.pdf (accessed on 1 March 2019).

[28] J. Nedoma, M. Fajkus, R. Martinek, H. Nazeran, P. Siska, Sensors, **17**, 1 (2017).

[29] J. Nedoma, S. Kepak, M. Fajkus, J. Cubik, P. Siska, R. Martinek, P. Krupa, Sensors, **18**, 11 (2018).

[30] J. Nedoma, M. Fajkus, S. Kepak, J. Cubik, R. Kahankova, P. Janku, V. Vasinek, H. Nazeran, R. Martinek, Advances in Electrical and Electronic Engineering **15**, 544 (2017).

[31] J. M. Bland, D. G. Altman, Statistical methods in
     laboratory medicine **8**, 135 (1999).
[32] P. Zhang, S. Ye, Z. Huang, D. Jiaerken, S. Zhao,
     L. Zhang, J. Wu, A noninvasive continuous fetal heart
     rate monitoring system for mobile healthcare based
     on fetal phonocardiography, (2019).
[33] L. Dziuda, M. Krej, F. W. Skibniewski, IEEE Sensors
     Journal **13**(12), 4986 (2013).
[34] C. J. Deepu, Z. Chen, J. T. Teo, S. H. Ng, X. Yang,
     Y. Lian, IEEE Biomedical Circuits and Systems
     Conference: Intelligent Biomedical Electronics and
     Systems for Better Life and Better Environment,
     BioCAS 2012 - Conference Publications, 53 (2012).

[35] Z. Chen, D. Lau, J. T. Teo, S. H. Ng, X. Yang,
     P. L. Kei, Journal of Biomedical Optics **19,** 5 (2014).
[36] J. Nedoma, M. Fajkus, R. Martinek, L. Bednarek,
     S. Zabka, D. Hruby, J. Jaros, V Vasinek, Proceedings
     of SPIE - The International Society for Optical
     Engineering **10231**, art. no. 1023119 (2017).

_____

[*]Corresponding author: jan.nedoma@vsb.cz